UCRL 231

UNIVERSITY OF CALIFORNIA

Radiation Laboratory

BERKELEY, CALIFORNIA

UCRL-8231

UNIVERSITY OF CALIFORNIA

Radiation Laboratory
Berkeley, California

Contract No. W-7405-eng-48

$\bar{p}$-p ELASTIC AND CHARGE-EXCHANGE SCATTERING AT ABOUT 120 Mev

Lewis E. Agnew, Jr., Tom Elioff, William B. Fowler, Louis Gilly, Richard L. Lander, Larry Oswald, Wilson M. Powell, Emilio Segrè, Herbert M. Steiner, Howard S. White, Clyde Wiegand and Tom Ypsilantis

March 28, 1958

Printed for the U. S. Atomic Energy Commission

$\bar{p}$-p ELASTIC AND CHARGE-EXCHANGE SCATTERING AT ABOUT 120 Mev

Lewis E. Agnew, Jr., Tom Elioff, William B. Fowler, Louis Gilly, Richard L. Lander, Larry Oswald, Wilson M. Powell, Emilio Segrè, Herbert M. Steiner, Howard S. White, Clyde Wiegand and Tom Ypsilantis

Radiation Laboratory
University of California
Berkeley, California

March 28, 1958

Observation of antiprotons in a propane or hydrogen bubble chamber offers the possibility of studying several phenomena for which counter or photographic emulsion techniques are less suitable.

Because there is a high ratio of pions, muons, and electrons to antiprotons in the available momentum-analyzed beams, these beams cannot be used in the bubble chamber without an initial purification, which increases the ratio of antiprotons to other particles. Such a purification has been achieved by utilizing the difference in rates of momentum loss in absorbers between antiprotons and other particles. The principle of the method is to pass a momentum-analyzed beam through an absorber. Since particles of unequal mass do not have the same specific ionization they lose different amounts of momentum, and a further magnetic deflection suffices to separate the particles physically according to mass. In this experiment a desirable momentum for antiprotons entering the bubble chamber was 684 Mev/c; however, at this momentum the ratio of undesirable particles to antiprotons at the target where they are produced is about 6×10^5. By starting with 970-Mev/c particles at the target and using the method of differential absorption, we decreased the ratio of undesirable particles (87% μ^-, 10% π^-, 3% e^-) to antiprotons entering the bubble chamber at 684 Mev/c to 1.5×10^4. A system of counters indicated when an antiproton entered the bubble chamber, and although the chamber was expanded on every Bevatron pulse, the lights were flashed and the chamber photographed only when an antiproton entered.

The chamber is 30 inches along the beam direction, 20 inches transverse to the beam, and 6.5 inches deep. It was filled with liquid propane of density 0.42 g/cm^3. Antiprotons entering the chamber with a momentum of 684 Mev/c had an average range of 21 inches in propane; however, approximately 40% of the antiprotons never came to rest but annihilated in flight.

We have observed 478 antiprotons entering the chamber. One such event is shown in Fig. 1. The complete analysis of these events is in progress; however, a preliminary report on the $\bar{p}$-p elastic scattering is now available. A total of 33 $\bar{p}$-p elastic collisions have been observed over a path length of 179 meters.[1] The scattering events occur between 30 and 215 Mev, with an

average energy of 120 Mev. Only $\bar{p}$-p scatterings with angles $\geq 7.5^{\circ}$ (lab) were identifiable because otherwise the energy of the recoil proton was too small to make a visible track and the scatterings were therefore indistinguishable from $\bar{p}$-C. A histogram showing the angular distribution of the scattering is given in Fig. 2 and, for comparison, a curve showing the result of a calculation by Fulco[2] based on the Ball-Chew[3] model. The angular distributions are similar, with a notable preponderance of forward scattering, which is reasonably interpreted as the diffraction scattering connected with the annihilation. These angular distributions differ markedly from that for n-p, which is also plotted for comparison. The total $\bar{p}$-p elastic cross section for scattering between 15° and 165° (c.m.) is 41 ± 19 mb. This should be compared with Fulco's value of 68 mb for the same angular interval.

The charge-exchange process $\bar{p} + p \rightarrow \bar{n} + n$ can be observed in the bubble chamber. One event has been identified and it is shown in Fig. 3 because of its inherent interest. The angle between the antiproton direction and the line connecting the antiproton ending with the vertex of the star is 30° (lab). The visible energy release in the star is $\gtrsim 1500$ Mev; the tentative identification of the annihilation products is 3 π^+ and 2 π^-. Thus the star is consistent with the process $\bar{n} + p \rightarrow 3\,\pi^+ + 2\,\pi^-$. The energy of the antiproton at the point of disappearance is estimated as 50 ± 30 Mev.

Other results, such as the carbon annihilation and scattering cross sections and details of the annihilation process, must await completion of the analysis.

References

1. Five additional $\bar{p}$-p scattering events have been observed in nuclear emulsions by Chamberlain, Goldhaber, Jauneau, Kalogeropoulos, Segre, and Silberberg. These are reported in the proceedings of the Padua Conference (1957).

2. Jose R. Fulco, Phys. Rev. (in press) and Theoretical Angular Distribution of Nucleon-Antinucleon Scattering at 140 Mev, UCRL-8183, Feb. 1958.

3. Ball and Chew, Phys. Rev. 109, 1385 (1958).

4. Wilmot N. Hess, A Summary of High-Energy Nucleon-Nucleon Cross-Section Data, UCRL-4639, Jan. 1956.

Figure Captions

Fig. 1. $\bar{p}$-p Scatterings. The antiproton (denser track) enters from the top, left of center. At an energy of 117 Mev, the antiproton scatters 41^0 to its left(in this photo, the viewer's right) from a proton. The recoil proton has a range of 4.4 cm (49 Mev). The scattered antiproton comes to rest in 8.3 cm (68 Mev) and annihilates on a carbon nucleus, showing five visible prongs.

Fig. 2. $\bar{p}$-p Elastic Scattering at 120 Mev. The histogram shows the angular distribution of 33 observed $\bar{p}$-p scattering events between 15^o and 165^o (c.m.) The dashed curve is the angular distribution calculated by Fulco. The n-p angular distribution is also shown for about the same energy.[4]

Fig. 3. An Antiproton Charge Exchange. The antiproton is incident from the top, left of center, and the antiproton ending is indicated by an arrow. The antineutron from the charge-exchange process annihilates in the lower center of the picture. Five pions are produced in the annihilation, with an energy release $>$ 1500 Mev.

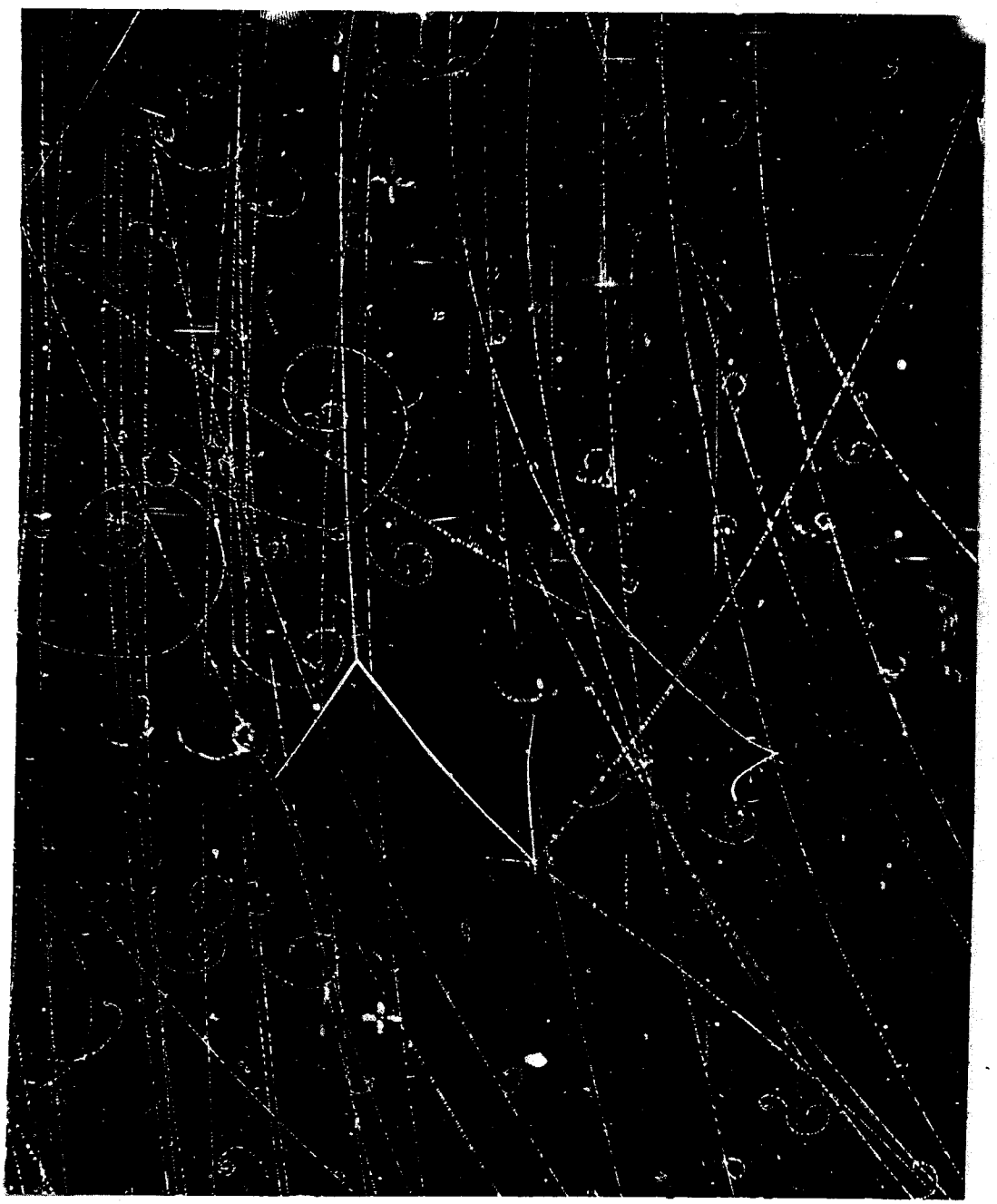

ZN-1929

Fig. 1

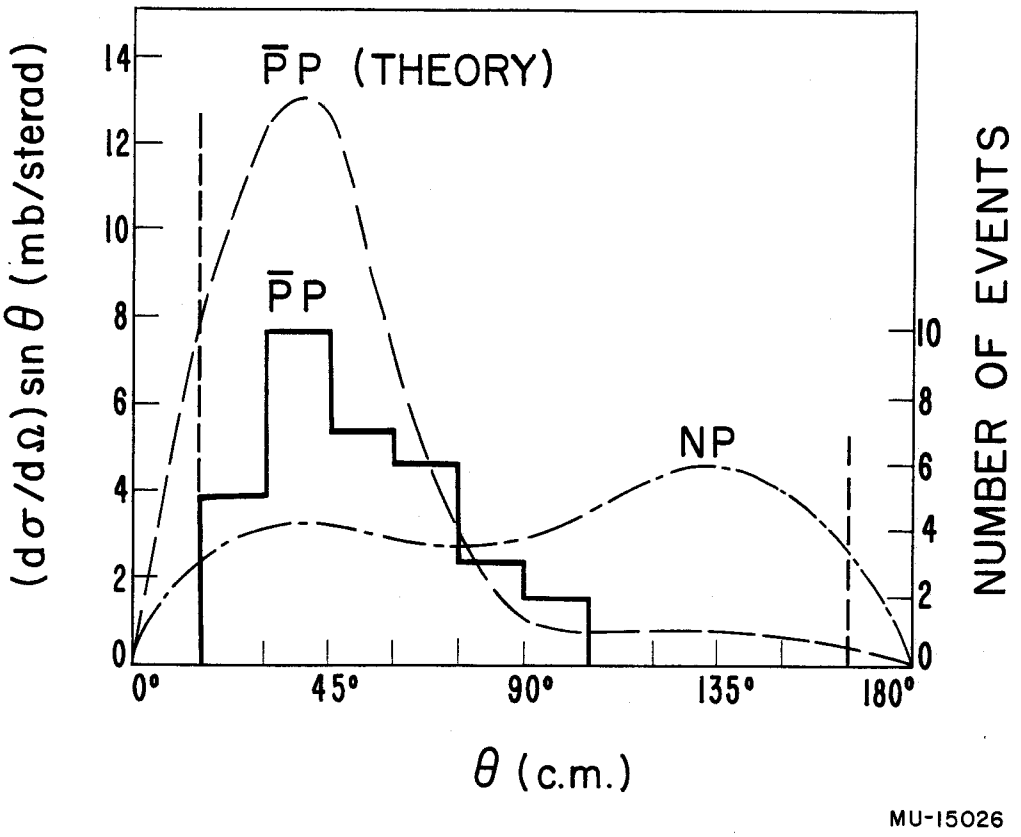
$\bar{P}P$ (THEORY)
$\bar{P}P$
NP
$(d\sigma/d\Omega)\sin\theta$ (mb/sterad)
NUMBER OF EVENTS
θ (c.m.)
0°
45°
90°
135°
180°
0
2
4
6
8
10
12
14
MU-15026

Fig. 2

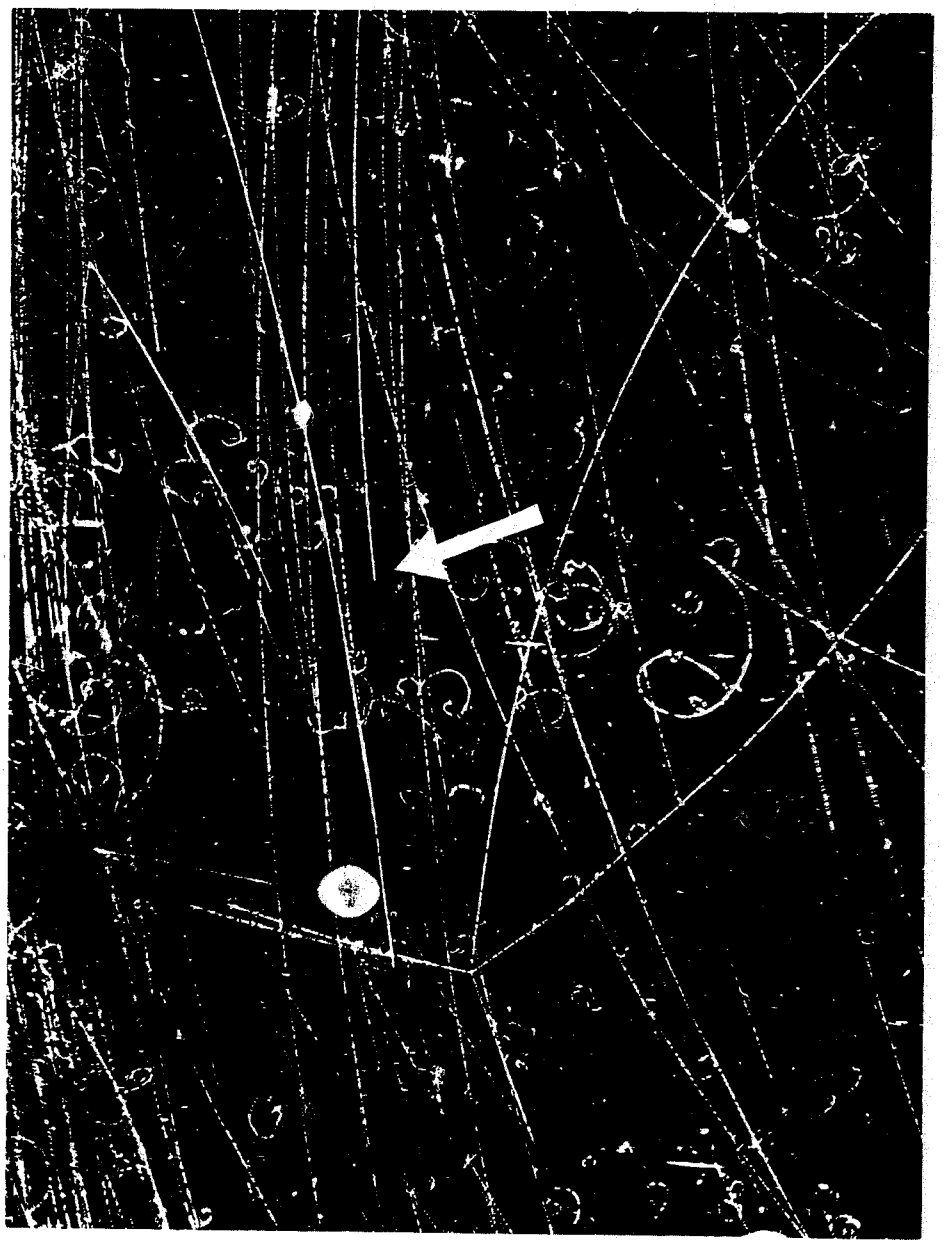

ZN-1930

Fig. 3